

Predict PPG Values of COVID Period (using the pre-COVID data as the baseline) Applying the Higher Order Equations of Interpolation Perturbation Theory from Quantum Mechanics and Carbs/Sugar Intake Amount as the Perturbation Factor Based on GH-Method: Math-Physical Medicine (No. 462)

Gerald C Hsu

EclaireMD Foundation, USA

***Corresponding author**

Gerald C Hsu, EclaireMD Foundation, USA

Submitted: 16 July 2021; Accepted: 23 July 2021; Published: 06 Aug 2021

Citation: Gerald C Hsu (2021) Predict PPG Values of COVID Period (using the pre-COVID data as the baseline) Applying the Higher Order Equations of Interpolation Perturbation Theory from Quantum Mechanics and Carbs/Sugar Intake Amount as the Perturbation Factor Based on GH-Method: Math-Physical Medicine (No. 462). *J App Mat Sci & Engg Res*, 5(2), 1-6.

Abstract

In this research note, the author applies the methodology of higher-order interpolation perturbation theory from quantum mechanics on his medical research work. This perturbation theory application includes the first-order, second-order, and third-order, to generate three predicted PPG waveforms with different prediction accuracies. He then collects two separate measured postprandial plasma glucose (PPG) data and their synthesized waveforms generated for two periods, pre-COVID (5/5/2018 - 1/18/2020) and COVID (1/19/2020 - 6/7/2021), as two baselines for comparison between predicted PPG data and waveforms (using pre-COVID as the baseline) and the measured COVID PPG data and waveform.

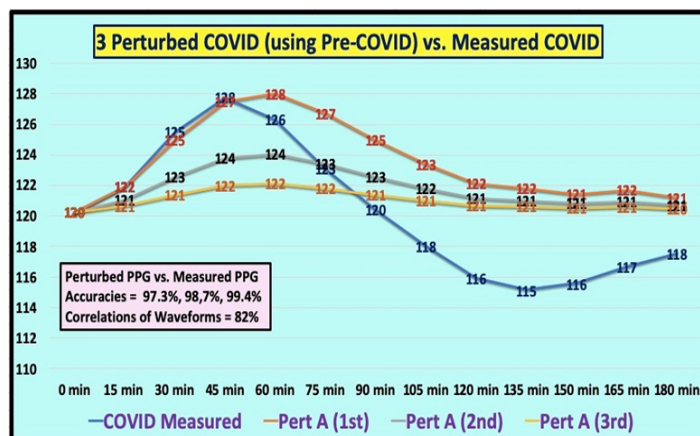
There are two final yardsticks to check in this study. The first target is to verify the prediction accuracies of these three perturbed PPG values. The second target is to examine the waveform similarity via calculated correlation coefficients between the measured PPG dataset or waveform and the three perturbed PPG datasets or waveforms.

The main purpose is to examine the prediction accuracy and waveform similarities in his current or future period of glucoses by using three different orders of perturbation equations based on the glucose data from the previous period as the prediction baseline.

In summary, the obvious conclusion drawn from this research work is that the perturbation equation provides a predicted PPG with high accuracy and duplicative waveform shapes. As a matter of fact, the higher-order of the perturbation equation used, the better results can be achieved for prediction accuracy. In this study, the first-order perturbation offers 97.3% prediction accuracy, the second-order perturbation provides 98.7% prediction accuracy, and the third-order perturbation delivers 99.4% prediction accuracy. All three perturbed PPG waveforms have equal level of waveform shape similarity with 81% versus the measured COVID PPG waveform. The lower than 90+% correlations are due to the selection of the pre-COVID PPG data as his calculation baseline.

In the real world, there are very few diabetes doctors and patients who can understand the perturbation theory of quantum mechanics, let alone be able to apply this theory on calculation of predicted future glucose based on previous data with a desired high

prediction accuracy.



Introduction

In this research note, the author applies the methodology of higher-order interpolation perturbation theory from quantum mechanics on his medical research work. This perturbation theory application includes the first-order, second-order, and third-order, to generate three predicted PPG waveforms with different prediction accuracies. He then collects two separate measured postprandial plasma glucose (PPG) data and their synthesized waveforms generated for two periods, pre-COVID (5/5/2018 - 1/18/2020) and COVID (1/19/2020 - 6/7/2021), as two baselines for comparison between predicted PPG data and waveforms (using pre-COVID as the baseline) and the measured COVID PPG data and waveform.

There are two final yardsticks to check in this study. The first target is to verify the prediction accuracies of these three perturbed PPG values. The second target is to examine the waveform similarity via calculated correlation coefficients between the measured PPG dataset or waveform and the three perturbed PPG datasets or waveforms.

The main purpose is to examine the prediction accuracy and waveform similarities in his current or future period of glucoses by using three different orders of perturbation equations based on the glucose data from the previous period as the prediction baseline.

Methods

The author has chosen not to repeat all of the details regarding his applied methods as described in other papers. Instead, he outlines a few important equations, formulas, or conditions in this article.

MPM Background

To learn more about his developed GH-Method: math-physical medicine (MPM) methodology, readers can read the following three papers selected from the published 400+ medical papers.

The first paper, No. 386 (Reference 1) describes his MPM methodology in a general conceptual format. The second paper, No. 387 (Reference 2) outlines the history of his personalized diabetes research, various application tools, and the differences between biochemical medicine (BCM) approach versus the MPM approach. The third paper, No. 397 (Reference 3) depicts a general flow diagram containing ~10 key MPM research methods and different tools.

Higher-Order Interpolation Perturbation Theory

The author applies the higher-order interpolation perturbation method to obtain his three “perturbed PPG” waveforms based on one function of the selected carbs/sugar intake amount functioning as the perturbation factors, that is the “Slope Equation”. He uses the “measured PPG” waveform as his “reference waveform”.

The following polynomial function is used as the perturbation equation:

$$A = f(x) \\ = A_0 + (A_1 * x) + (A_2 * x^{**2}) + (A_3 * x^{**3}) + \dots + (A_n * x^{**n})$$

Where A is the perturbed glucose, A_i is the measured glucose, and x is the “perturbation factor” based on different carbs/sugar intake amounts.

For this particular study, he choose his A_i where $i=1$ to 3. Therefore, the perturbation theory equation from above can be simplified to the following form:

$$A = f(x) \\ = A_0 + (A_1 * x) + (A_2 * x^{**2}) + (A_3 * x^{**3})$$

Or the third-order interpolation perturbation equation can then be expressed in the following general format:

$$Y_i \\ = Y_1 + (\text{slope } 1) * (Y_2 - Y_1) + (\text{slope } 2) * (Y_2 - Y_1) + (\text{slope } 3) * (Y_2 - Y_1)$$

More specifically, the following formats of three perturbation equations are utilized in the calculations of this study:

$$Y \text{ of first order} = (Y_2 - Y_1) * (\text{slope } 1)$$

$$Y \text{ of second order} = (Y_2 - Y_1) * (\text{slope } 2)$$

$$Y \text{ of third order} = (Y_2 - Y_1) * (\text{slope } 3)$$

Where:

Y_1 = original glucose Y at time 1

Y_2 = advanced glucose Y at time 2

$(Y_2 - Y_1)$ = (Glucose Y at Time 2 - Glucose Y at Time 1)

The perturbation factor of **Slope** is an arbitrarily selected parameter that controls the size of the perturbation. The author has chosen a function of carbs/sugar intake amount, as his perturbation factor or slope, which is further defined as follows:

In this particular study, he selects the 4.9 grams as his low-bound carbs/sugar and 21.8 grams as his high-bound carbs/sugar, while 13.2 grams as his selected carbs/sugar amount.

The equations for 3 slopes are:

$$\text{Slope } 1 \\ = (\text{Selected Carbs} - \text{Low-bound Carbs}) / (\text{High-bound Carbs} - \text{Low-bound Carbs})$$

$$\text{Slope } 2 \\ = (\text{Slope } 1 * \text{Slope } 1) \\ \text{or } (\text{Slope }^{**2})$$

$$\text{Slope } 3 \\ = (\text{Slope } 1 * \text{Slope } 1 * \text{Slope } 1) \\ \text{or } (\text{Slope }^{**3})$$

It should be noted that, for achieving a better predicted glucose value, the selected carbs amount should be within the range of the high-bound carbs and the low-bound carbs, where these two boundary carbs amounts should be within 4x in magnitude to each other.

Therefore, in this particular study, his three slope values are calculated as follows:

$$\text{Slope } 1 = 0.53$$

Slope 2 = 0.28
Slope 3 = 0.15

Results

Figure 1 shows the background information of PPG for both pre-COVID period and COVID period.



Figure 1: Two baseline periods of Pre-COVID (5/5/2018 - 1/18/2020) and COVID (1/19/2020 - 6/7/2021)

Figure 2 reflects his input data and valuation results of this study.

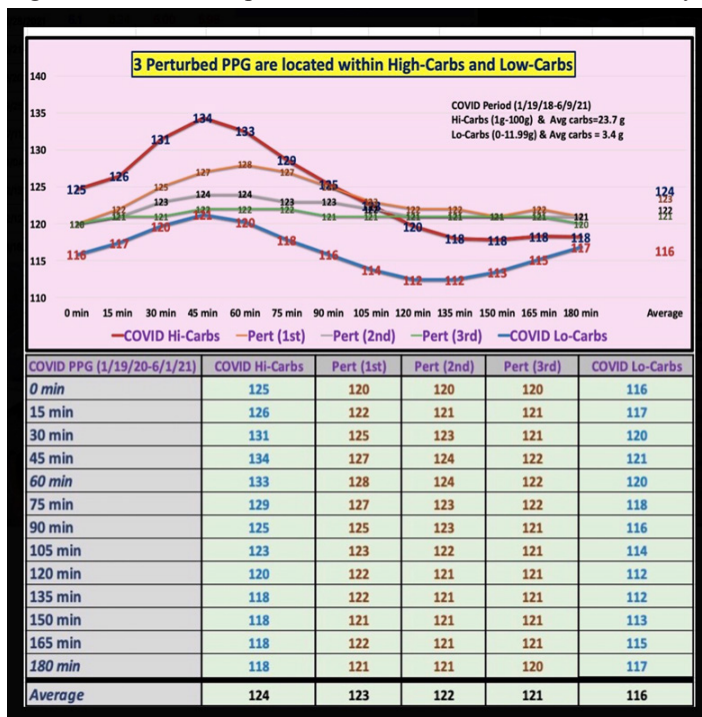


Figure 2: 3 Perturbed PPG curves and 1 measured PPG curve for both pre-COVID period (5/5/2018 - 1/18/2020) and COVID period (1/19/2020 - 6/7/2021)

In Figures 1 and 2, we should pay attention to certain key data and curve characteristics of these two PPG waveforms which are described below.

The peak PPG values around 45-minutes to 60-minutes are 145 mg/dL for the pre-COVID period and 128 mg/dL for the COVID period. The pre-COVID PPG waveform is gradually declining after 75-minutes all the way to 180-minutes, but the COVID PPG waveform has a curve tilting-upward point at 135-minutes.

Figure 3 assembles the pre-COVID and COVID PPG waveforms into one graphic diagram. Therefore, the different peak values as well as the waveform tilting upward at 135-minutes of the COVID period are clearly observed. The author conducted three different orders of perturbation for both periods using each period's measured PPG data as their baseline data. Therefore, both periods have demonstrated extremely high prediction accuracies (>99.8%) and waveform shape similarities (>90.0%).

PPG (1/19/20-6/1/21)	COVID Measured	Pert A (1st)	Pert A (2nd)	Pert A (3rd)	Pre-COVID Measured
0 min	120	120	120	120	129
15 min	122	122	121	121	133
30 min	125	125	123	121	139
45 min	128	127	124	122	144
60 min	126	128	124	122	145
75 min	123	127	123	122	142
90 min	120	125	123	121	139
105 min	118	123	122	121	136
120 min	116	122	121	121	133
135 min	115	122	121	121	132
150 min	116	121	121	121	132
165 min	117	122	121	121	132
180 min	118	121	121	120	131
Average	120.3	123.5	121.8	121.0	135.8
Prediction Accuracy	Perturbed vs. COVID Measured	97.3%	98.7%	99.4%	
Correlation	Perturbed vs. COVID Measured	81%	81%	81%	
Carbs & Walking	High-carbs	Selected-total	Low-carbs	Conversion Factor	
Selection of Carbs	21.8	13.2	4.9	0.93	
Perturbation Theory		1st order	2nd order	3rd order	
(Select-Low)/(High-Low) Slope		0.49	0.24	0.12	

Figure 3: Table of input data and calculation results of 3 perturbed PPG (using pre-COVID measured data as their baselines) versus the measured PPG of COVID period

It should be noted again that he has chosen the selected carbs of 13.2 grams, which is his actual measured carbs/sugar amount in the COVID period, located approximately in the middle point of the low-bound carbs of 4.9 grams and high-bound carbs of 21.8 grams. His three calculated slopes are 0.53 for the first-order perturbation, 0.28 for the second-order perturbation, and 0.15 for the third-order perturbation.

Figure 4 depicts the ending result of the COVID predicted PPG using the pre-COVID data as his calculation baseline.

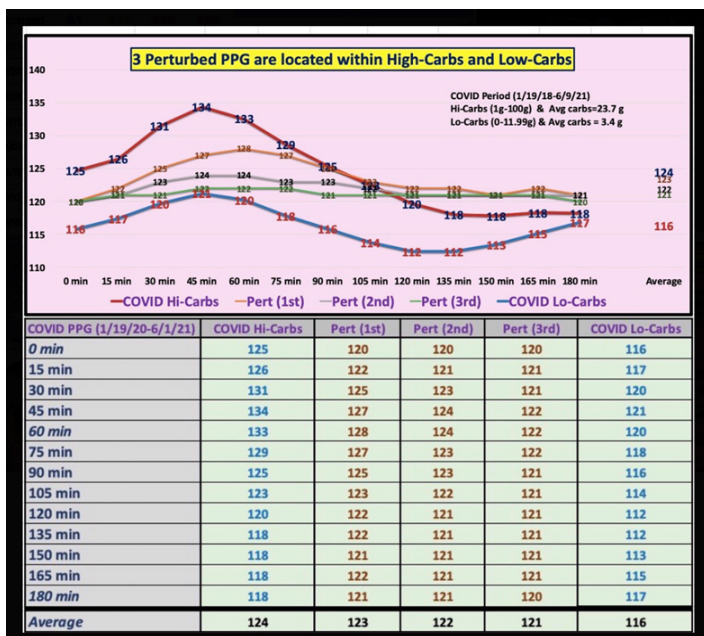


Figure 4: Comparison of 3 perturbed PPG waveforms (using the pre-COVID measured data as their baselines) versus the measured PPG waveform of COVID period (1/19/2020 - 6/7/2021)

The average PPG value and prediction accuracy of each perturbation equation for the COVID period are listed below:

Measured: 120.3 mg/dL, 100%
First-order: 123.5 mg/dL, 97.3%
Second-order: 121.8 mg/dL, 98.7%
Third-order: 121.0 mg/dL, 99.4%

All three perturbed waveform predictions have the same shape similarity (i.e., same correlation coefficients of $R=81\%$) in comparison against the measured COVID PPG. The slightly lower than 90% of R is due to the fact that the 3 predicted COVID waveforms are using the pre-COVID measured data as their baseline of calculation. Nevertheless, an 81% correlation is still considered as an extremely high number in terms of waveform shape similarity comparison.

The mathematical power of achieving excellent approximation of PPG values and their corresponding waveforms by using perturbation theory can be detected clearly via the summarized table shown below in the format of first-order, second-order, third-order:

Correlation: 81%, 81%, 81%
Accuracy: 97.3%, 98.7%, 99.4%

Figure 5 further demonstrates the comparison of 3 perturbed PPG waveforms versus both of measured PPG from High-Carbs and measured PPG from Low-Carbs of COVID period (1/19/2020 - 6/9/2021). It is quite obviously that all of these three perturbed COVID PPG curves are located within the boundary of high-carbs PPG curve and low carbs PPG curve despite of they were generated using pre-COVID PPG data as their baselines.

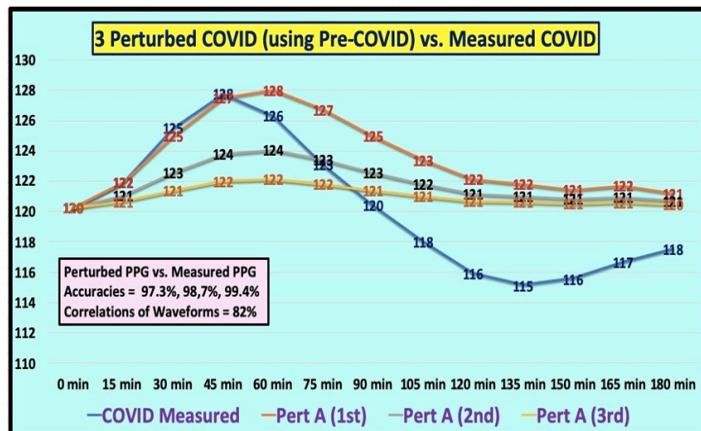


Figure 5: Comparison of three perturbed PPG waveforms versus both of measured PPG from High-Carbs and measured PPG from Low-Carbs of COVID period (1/19/2020 - 6/9/2021)

Conclusions

In summary, the obvious conclusion drawn from this research work is that the perturbation equation provides a predicted PPG with high accuracy and duplicative waveform shapes. As a matter of fact, the higher-order of the perturbation equation used, the better results can be achieved for prediction accuracy. In this study, the first-order perturbation offers 97.3% prediction accuracy, the second-order perturbation provides 98.7% prediction accuracy, and the third-order perturbation delivers 99.4% prediction accuracy. All three perturbed PPG waveforms have equal level of waveform shape similarity with 81% versus the measured COVID PPG waveform. The lower than 90+% correlations are due to the selection of the pre-COVID PPG data as his calculation baseline.

In the real world, there are very few diabetes doctors and patients who can understand the perturbation theory of quantum mechanics, let alone be able to apply this theory on calculation of predicted future glucose based on previous data with a desired high prediction accuracy [1-37].

References

- Hsu Gerald C (2021) Biomedical research using GH-Method: math-physical medicine, version 3 (No. 386).
- Hsu Gerald C (2021) From biochemical medicine to math-physical medicine in controlling type 2 diabetes and its complications (No. 387).
- Hsu Gerald C (2021) Methodology of medical research: Using big data analytics, optical physics, artificial intelligence, signal processing, wave theory, energy theory and transforming certain key biomarkers from time domain to frequency domain with spatial analysis to investigate organ impact by relative energy associated with various medical conditions (No. 397).
- Hsu Gerald C (2021) Linear relationship between carbohydrates & sugar intake amount and incremental PPG amount via engineering strength of materials using GH-Method: math-physical medicine, Part 1 No. 346.
- Hsu Gerald C (2021) Investigation on GH modulus of linear elastic glucose with two diabetes patients data using

- GH-Method: math-physical medicine, Part 2 No. 349.
6. Hsu Gerald C (2021) Investigation of GH modulus on the linear elastic glucose behavior based on three diabetes patients' data using the GH-Method: math-physical medicine, Part 3 No. 349.
 7. Hsu Gerald C (2021) Coefficient of GH.f-modulus in the linear elastic fasting plasma glucose behavior study based on health data of three diabetes patients using the GH-Method: math-physical medicine, Part 4 No. 356. *J App Mat Sci & Engg Res* 4: 50-55.
 8. Hsu Gerald C (2020) High accuracy of predicted postprandial plasma glucose using two coefficients of GH.f-modulus and GH.p-modulus from linear elastic glucose behavior theory based on GH-Method: math-physical medicine, Part 5 No. 357. *J App Mat Sci & Engg Res* 4: 71-76.
 9. Hsu Gerald C (2021) Improvement on the prediction accuracy of postprandial plasma glucose using two biomedical coefficients of GH-modulus from linear elastic glucose theory based on GH-Method: math-physical medicine, Part 6 No. 358.
 10. Hsu Gerald C (2021) High glucose predication accuracy of postprandial plasma glucose and fasting plasma glucose during the COVID-19 period using two glucose coefficients of GH-modulus from linear elastic glucose theory based on GH-Method: math-physical medicine, Part 7 No. 359.
 11. Hsu Gerald C (2021) Investigation of two glucose coefficients of GH.f-modulus and GH.p-modulus based on data of 3 clinical cases during COVID-19 period using linear elastic glucose theory of GH-Method: math-physical medicine, Part 8 No. 360.
 12. Hsu Gerald C (2020) Postprandial plasma glucose lower and upper boundary study using two glucose coefficients of GH-modulus from linear elastic glucose theory based on GH-Method: math-physical medicine, Part 9 No. 361. *J App Mat Sci & Engg Res* 4: 83-87.
 13. Hsu Gerald C (2020) Six international clinical cases demonstrating prediction accuracies of postprandial plasma glucoses and suggested methods for improvements using linear elastic glucose theory of GH-Method: math-physical medicine, Part 10 No. 362. *J App Mat Sci & Engg Res* 4: 88-91.
 14. Hsu Gerald C (2021) A special Neuro-communication influences on GH.p-modulus of linear elastic glucose theory based on data from 159 liquid egg and 126 solid egg meals using GH-Method: math-physical medicine, Part 11 No. 363. *J App Mat Sci & Engg Res* 5: 126- 131.
 15. Hsu Gerald C (2020) GH.p-modulus study of linear elastic glucose theory based on data from 159 liquid egg meals, 126 solid egg meals, and 2,843 total meals using GH-Method: math-physical medicine, Part 12 No. 364. *J App Mat Sci & Engg Res* 4: 31-36.
 16. Hsu Gerald C (2020) Detailed GH.p-modulus values at 15-minute time intervals for a synthesized sensor PPG waveform of 159 liquid egg meals, and 126 solid egg meals using linear elastic glucose theory of GH-Method: math-physical medicine, Part 13 No. 365. *J App Mat Sci & Engg Res* 4: 37-42.
 17. Hsu Gerald C (2020) A lifestyle medicine model for family medical practices based on 9-years of clinical data including food, weight, glucose, carbs/sugar, and walking using linear elastic glucose theory and GH-Method: math-physical medicine (Part 14) No. 367. *MOJ Gerontol Ger* 5: 197-204.
 18. Hsu Gerald C (2020) GH.p-modulus study during 3 periods using finger-piercing glucoses and linear elastic glucose theory (Part 15) of GH-Method: math-physical medicine No. 369. *J App Mat Sci & Engg Res* 4:31-36.
 19. Hsu Gerald C (2020) GH.p-modulus study using both finger and sensor glucoses and linear elastic glucose theory (Part 16) of GH-Method: math-physical medicine (No. 370). *J App Mat Sci & Engg Res* 4: 62-64.
 20. Hsu Gerald C (2020) A summarized investigation report of GH.p-modulus values using linear elastic glucose theory of GH-Method: math-physical medicine, Part 17 No. 371. *J App Mat Sci & Engg Res* 5: 113-118.
 21. Hsu Gerald C (2021) An experimental study on self-repair and recovery of pancreatic beta cells via carbs/sugar intake increase and associated postprandial plasma glucose variation using linear elastic glucose theory (part 18) and GH-Method: math-physical medicine No. 396.
 22. Hsu Gerald C (2021) Analyzing roles and contributions of fasting plasma glucose, carbs/sugar intake amount, and post-meal walking steps on the formation of postprandial plasma glucose using Linear Elastic Glucose Theory of GH-Method: math-physical medicine, LEGT Part 19 No. 401.
 23. Hsu Gerald C (2021) Analyzing relations among weight, FPG, and PPG using statistical correlation analysis and Linear Elastic Glucose Theory of GH-Method: math-physical medicine, LEGT Part 20 No. 402.
 24. Hsu, Gerald C (2021) Estimating cardiovascular disease risk and insulin resistance via transforming glucose wave fluctuations from time domain into associated energy in frequency domain and applying the linear elastic glucose theory of GH-Method: math-physical medicine, LEGT Part 21 No. 403.
 25. Hsu Gerald C (2021) PPG magnitude and fluctuation study of three 346-days periods using time-domain and frequency domain analyses as well as linear elastic glucose theory (part 22) of GH-Method: math-physical medicine No. 411.
 26. Hsu Gerald C (2021) Using 12-years glucoses including intermittent fasting glucose data, and high-carbs meals glucose data to study the suitability, lower-bound, and upper-bound of the linear elastic glucose theory based on GH-Method: math-physical medicine, Part 23 (No. 412).
 27. Hsu Gerald C (2021) A case study of pre-virus period versus virus period applying wave theory, energy theory, Fourier transform, and linear elastic glucose theory (LEGT Part 24) to estimate risk probability of having a cardiovascular disease or stroke and achieving longevity based on GHMethod: math-physical medicine (No. 413).
 28. Hsu Gerald C (2021) A case study of three time periods applying wave theory, energy theory, Fourier transform, and linear elastic glucose theory (LEGT Part 25) to estimate risk probability of having a cardiovascular disease or stroke and achieving longevity based on GH-Method: math-physical medicine (No. 414).
 29. Hsu Gerald C (2021) A summary report of 25 research articles utilizing linear elastic glucose theory based on GH-Method: math-physical medicine, LEGT Part 26 (No. 415).
 30. Hsu Gerald C (2021) An artificial intelligence model apply-

-
- ing linear elastic glucose theory to control diabetes and its complications to achieve longevity based on GH-Method: math-physical medicine, LEGT Part 27 (No. 416).
31. Hsu Gerald C (2017) Three GH-modulus for predicted glucose via LEGT linear PPG and HbA1C control based on 12-years lifestyle data and finger-pierced glucoses using GH-Method: math-physical medicine, LEGT Part 28 (No. 417).
 32. Hsu Gerald C (2020) Applying first-order perturbation theory of quantum mechanics to predict and build a postprandial plasma glucose waveform (GH-Method: math-physical medicine) No. 152. Journal of Geriatric Research 4: 1-2.
 33. Hsu Gerald C (2020) Applying the first-order interpolation perturbation method to establish predicted PPG waveforms based on carbs/sugar intake amounts using GH-Method: math-physical medicine (No.154). J App Mat Sci & Engg Res 4: 65-70.
 34. Hsu Gerald C (2021) Application of perturbation theory, frequency domain energy theory, and linear elasticity theory to study and predict postprandial plasma glucose behaviors and their impact on internal organs of Type 2 diabetes patients based on GH-Method: math-physical medicine (No. 423).
 35. Hsu Gerald C (2021) Application of perturbation theory and linear elasticity glucose theory (LEGT Part 31) on postprandial plasma glucose waveform of a single lunch based on GH-Method: math-physical medicine (No. 424).
 36. Hsu Gerald C (2021) Application of higher-order interpolation perturbation theory on postprandial plasma glucose waveform of a single lunch based on GH-Method: math-physical medicine (No. 426).
 37. Hsu Gerald C (2021) Application of the first, second, and third order equations of interpolation perturbation theory from quantum mechanics to predict a synthesized 3-year postprandial plasma glucose wave based on GH-Method: math-physical medicine (No. 460).

Copyright: ©2021 Gerald C Hsu. This is an open-access article distributed under the terms of the Creative Commons Attribution License, which permits unrestricted use, distribution, and reproduction in any medium, provided the original author and source are credited.